

# Nonparametric Bayesian Deep Networks with Local Competition

Konstantinos P. Panousis<sup>1</sup> Sotirios Chatzis<sup>2</sup> Sergios Theodoridis<sup>1</sup>

## Abstract

Local competition among neighboring neurons is a common procedure taking place in biological systems. This finding has inspired research on more biologically plausible deep networks that comprise competing linear units, as opposed to nonlinear units that do not entail any form of (local) competition. This paper revisits this modeling paradigm, with the aim of enabling inference of networks that retain state-of-the-art accuracy for the least possible model complexity; this includes the needed number of connections or locally competing sets of units, as well as the required floating-point precision for storing the network weights. To this end, we leverage solid arguments from the field of Bayesian nonparametrics. Specifically, we introduce auxiliary discrete latent variables of model component utility, and perform Bayesian inference over them. Then, we impose appropriate stick-breaking priors over the introduced discrete latent variables; these give rise to a well-established sparsity-inducing mechanism. As we experimentally show using benchmark datasets, our approach yields networks with less memory footprint than the state-of-the-art, and with no compromises in predictive accuracy.

## 1. Introduction

Deep neural networks (DNNs) (LeCun et al., 2015) are flexible models that represent complex functions as a combination of simpler primitives. Despite their success in a wide range of applications, they typically suffer from overparameterization: they entail millions of weights, a large fraction of which is actually redundant. This leads to unne-

cessary computational burden, and limits their scalability to commodity hardware devices. In addition, this fact renders them susceptible to strong overfitting tendencies that may severely undermine their generalization capacity.

The deep learning community has devoted significant effort to address overfitting in deep learning;  $\ell_2$  regularization, Dropout, and variational variants thereof are characteristic such examples (Gal & Ghahramani, 2015). However, the scope of regularization is limited to effectively training (and retaining) all network weights. Addressing redundancy in deep networks requires data-driven structure shrinkage and weight compression techniques.

A popular type of solution to this end consists in training a condensed student network by leveraging a previously trained full-fledged teacher network (Ba & Caruana, 2014; Hinton et al., 2015). However, this paradigm suffers from two main drawbacks: (i) One cannot avoid the computational costs and overfitting tendencies related to training a large deep network; on the contrary, the total training costs are augmented with the weight distillation and training costs of the student network; and (ii) the student teaching procedure itself entails a large deal of heuristics and assorted artistry in designing effective teacher distillation.

As an alternative, several researchers have examined application of network component (unit/connection) pruning criteria. In most cases, these criteria are applied on top of some appropriate regularization technique. In this context, Bayesian Neural Networks (BNNs) have been proposed as a full probabilistic paradigm for formulating DNNs (Gal & Ghahramani, 2015; Graves, 2011), obtained by imposing a prior distribution over their weights. Then, appropriate posteriors are inferred, and predictive distributions are obtained via marginalization in the Bayesian averaging sense. This way, BNNs induce strong regularization under a solid inferential framework. In addition, they naturally allow for reducing floating-point precision in storing the network weights. Specifically, since Bayesian inference boils down to drawing samples from an inferred weight posterior, the higher the inferred weight posterior variance, the lower the needed floating-point precision (Louizos et al., 2017).

Finally, Chatzis (2018) recently considered addressing these problems by introducing an additional set of auxiliary Bernoulli latent variables, which explicitly indicate the util-

<sup>1</sup>Department of Informatics and Telecommunications, National And Kapodistrian University of Athens, Greece

<sup>2</sup>Department of Electrical Eng., Computer Eng., and Informatics Cyprus University of Technology, Cyprus. Correspondence to: Konstantinos P. Panousis <kpanousis@di.uoa.gr>, Sotirios Chatzis <sotirios.chatzis@cut.ac.cy>, Sergios Theodoridis <stheodor@di.uoa.gr>.

ity of each component (in an “on/off” fashion). In this context, they obtain a sparsity-inducing behavior, by imposing appropriate stick-breaking priors (Ishwaran & James, 2001) over the postulated auxiliary latent variables. Their study, although limited to variational autoencoders, showed promising results in a variety of benchmarks.

On the other hand, a prevalent characteristic of modern deep networks is the use of nonlinear units on each hidden layer. Even though this sort of functionality offers a mathematically convenient way of creating a hierarchical model, it is also well understood that it does not come with strong biological plausibility. Indeed, there is an increasing body of evidence supporting that neurons in biological systems that have similar functional properties are aggregated together in modules or columns where local competition takes place (Kandel et al., 1991; Andersen et al., 1969; Eccles et al., 1967; Stefanis, 1969; Douglas & Martin, 2004; Lansner, 2009). This is effected via the entailed lateral inhibition mechanisms, under which only a single neuron within a block can be active at a steady state.

Drawing from this inspiration, several researchers have examined development of deep networks which replace nonlinear units with local competition mechanisms among simpler linear units. As it has been shown, such local winner-takes-all (LWTA) networks can discover effective sparsely distributed representations of their input stimuli (Lee & Seung, 1999; Olshausen & Field, 1996), and constitute universal function approximators, as powerful as networks with threshold or sigmoidal units (Maass, 1999; 2000). In addition, this type of network organization has been argued to give rise to a number of interesting properties, including automatic gain control, noise suppression, and prevention of catastrophic forgetting in online learning settings (Srivastava et al., 2013; Grossberg, 1988; McCloskey & Cohen, 1989).

This paper draws from these results, and attempts to offer a principled paradigm for network pruning and weight compression in the context of biologically-inspired LWTA-based deep networks. We posit that the capacity to infer an explicit posterior distribution of component (connection/unit) utility in the context of LWTA-based deep networks may offer significant advantages in model effectiveness and computational efficiency. The proposed inferential construction relies on nonparametric Bayesian inference arguments, namely stick-breaking priors; we employ these tools in a fashion tailored to the unique structural characteristics of LWTA networks. This way, we give rise to a data-driven mechanism that intelligently adapts model structure and infers the needed floating-point precision.

We derive efficient training and inference algorithms for our model, by relying on stochastic gradient variational Bayes (SGVB). We dub our approach Stick-Breaking LWTA

(SB-LWTA) networks. We evaluate our approach using well-known benchmark datasets. Our provided empirical evidence vouches for the capacity of our approach to yield predictive accuracy at least competitive with the state-of-the-art, while shrinking a trained network and its memory footprint much better than the competition.

The remainder of this paper is organized as follows: In Section 2, we briefly present some necessary theoretical background. In Section 3, we introduce the proposed approach, and elaborate on its training and inference algorithms. In Section 4, we perform an extensive experimental evaluation of our approach, and provide insights into its functionality. Finally, in the concluding Section, we summarize the contribution of this work, and discuss directions for further research.

## 2. Theoretical Background

### 2.1. Indian Buffet Process

The Indian Buffet Process (IBP) (Griffiths & Ghahramani, 2005) is a probability distribution over infinite binary matrices. By using it as a prior, it allows for inferring how many latent features are needed for modeling a given set of observations, in a way that ensures sparsity in the obtained representations. In addition, it also allows for the emergence of new features as new observations appear. Teh et al. (2007) presented a stick-breaking construction for the IBP, which renders it amenable to variational inference. Let us consider  $N$  observations, and denote as  $\mathbf{Z} = [z_{i,k}]_{i,k=1}^{N,K}$  a binary matrix where each entry indicates the existence of feature  $k$  in observation  $i$ . Taking the infinite limit,  $K \rightarrow \infty$ , we arrive at the following hierarchical representation for the IBP (Teh et al., 2007):

$$u_k \sim \text{Beta}(\alpha, 1) \quad \pi_k = \prod_{i=1}^k u_i \quad z_{ik} \sim \text{Bernoulli}(\pi_k)$$

Here,  $\alpha > 0$  is the innovation parameter of the IBP, which controls the magnitude of the induced sparsity. In practice,  $K \rightarrow \infty$  denotes a setting whereby we obtain an overcomplete feature representation of the observed data; that is,  $K$  equals input dimensionality.

### 2.2. Stochastic Gradient Variational Bayes

In this paper, Bayesian inference is performed approximately via stochastic gradient maximization of the model evidence lower bound (ELBO). This is commonly referred to as Stochastic Gradient Variational Bayes (SGVB) (Kingma & Welling, 2014), and requires performing a Monte-Carlo (MC) approximation of the conditional log-likelihood posterior expectations entailed in the expression of the ELBO. As such an approximation results in estimators of prohibitively

high variance, one has to resort to some sort of variance reduction technique. A common solution to this end is the reparameterization trick, under which the drawn MC samples are expressed as differentiable transformations of low-variance noise variables  $\epsilon$  and the parameters of the sought posterior (Kingma & Welling, 2014). This is easily attainable when dealing with continuous latent variables, especially of elliptical form, e.g. Gaussians. Yet, it becomes harder when the continuous latent variables we are dealing with are of different form. Specifically, when it comes to models with IBP priors, the entailed Beta-distributed stick variables are not amenable to the reparameterization trick. To address this issue, one can approximate the Beta( $a_k, b_k$ )-distributed stick variables,  $u_k$ , via the Kumaraswamy distribution (Kumaraswamy, 1980):

$$p(u_k; a_k, b_k) = a_k b_k u_k^{a_k-1} (1 - u_k^{a_k})^{b_k-1} \quad (1)$$

Samples from this distribution can be reparameterized as follows (Nalisnick & Smyth, 2016):

$$u_k = \left(1 - (1 - X)^{\frac{1}{b_k}}\right)^{\frac{1}{a_k}}, \quad X \sim U(0, 1) \quad (2)$$

### 2.2.1. DEALING WITH DISCRETE LATENT VARIABLES

In the case of Discrete (Categorical or Bernoulli) latent variables, performing back-propagation through reparameterized drawn samples, as described above, becomes infeasible. Recently, the solution of introducing appropriate continuous relaxations has been proposed by different research teams (Jang et al., 2017; Maddison et al., 2017). Let  $\alpha \in (0, \infty)^K$  be the *unnormalized* probabilities of a considered Discrete distribution,  $\mathbf{X} = [X_k]_{k=1}^K$ , and  $\lambda \in (0, \infty)$  be a hyperparameter referred to as the *temperature* of the relaxation. Then, the drawn samples of  $\mathbf{X}$  are expressed as differentiable functions of the form:

$$X_k = \frac{\exp(\log \alpha_k + G_k)/\lambda}{\sum_{i=1}^K \exp((\log \alpha_i + G_i)/\lambda)}, \quad (3)$$

$$G_k = -\log(-\log U_k), \quad U_k \sim \text{Uniform}(0, 1) \quad (4)$$

In our work, the values of  $\lambda$  are annealed during training as suggested in Jang et al. (2017).

## 3. Proposed Approach

In this work, we consider a paradigm of designing deep networks whereby the output of each layer is derived from blocks of competing linear units, and appropriate arguments from nonparametric statistics are employed to infer network component utility in a Bayesian sense. An outline of the envisaged modeling rationale is provided in Fig. 1.

Let  $\{\mathbf{x}_n\}_{n=1}^N \in \mathbb{R}^J$  be an input dataset containing  $N$  observations, with  $J$  features each. Hidden layers in traditional neural networks contain nonlinear units; they are presented with linear combinations of the inputs, obtained via

a weights matrix  $\mathbf{W} \in \mathbb{R}^{J \times K}$ , and produce output vectors  $\{\mathbf{y}_n\}_{n=1}^N \in \mathbb{R}^K$  as input to the next layer. In our approach, this mechanism is replaced by the introduction of LWTA blocks in the hidden layers, each containing a set of competing linear units. The layer input is originally presented to each block, via different weights for each unit; thus, the weights of the connections are now organized into a three-dimensional matrix  $\mathbf{W} \in \mathbb{R}^{J \times K \times U}$ , where  $K$  denotes the number of blocks and  $U$  is the number of competing units therein.

Let us consider a layer of the proposed model. Within each block, the linear units compute their activations; then, the block selects one winner unit on the basis of a competitive random sampling procedure we describe next, and sets the rest to zero. This way, we yield a sparse layer output, encoded into the vectors  $\{\mathbf{y}_n\}_{n=1}^N \in \mathbb{R}^{K \cdot U}$  that are fed to the next layer. In the following, we encode the outcome of local competition between the units of each block via the discrete latent vectors  $\xi_n \in \text{one\_hot}(U)^K$ , where  $\text{one\_hot}(U)$  is an one-hot vector with  $U$  components. These denote the winning unit out of the  $U$  competitors in each of the  $K$  blocks of the layer, when presented with the  $n$ th datapoint.

To allow for inferring which layer connections must be retained, we adopt concepts from the field of Bayesian nonparametrics. Specifically, we commence by introducing a matrix of binary latent variables,  $\mathbf{Z} \in \{0, 1\}^{J \times K}$ . The  $(j, k)$ th entry therein is equal to one if the  $j$ th input is presented to the  $k$ th block, and equal to zero otherwise; in the latter case, the corresponding *set of weights*,  $\{w_{j,k,u}\}_{u=1}^U$ , are essentially removed from the model. Subsequently, we impose an IBP prior over  $\mathbf{Z}$ , to allow for performing inference over it, in a way that promotes sparsity, as explained in Section 2.1. Turning to the winner sampling procedure within each LWTA block, we postulate that the latent variables  $\xi_n$  are also driven from the layer input, and exploit the connection utility information encoded into the inferred  $\mathbf{Z}$  matrices.

Let us begin with defining the expression of layer output,  $\mathbf{y}_n \in \mathbb{R}^{K \cdot U}$ . Following the above-prescribed rationale, we have:

$$[\mathbf{y}_n]_{ku} = [\xi_n]_{ku} \sum_{j=1}^J (w_{j,k,u} \cdot z_{j,k}) \cdot [\mathbf{x}_n]_j \in \mathbb{R} \quad (5)$$

where we denote as  $[\mathbf{h}]_l$  the  $l$ th component of a vector  $\mathbf{h}$ . In this expression, we consider that the winner indicator latent vectors are drawn from a Categorical (posterior) distribution of the form:

$$q([\xi_n]_k) = \text{Discrete} \left( [\xi_n]_k \middle| \text{softmax} \left( \sum_{j=1}^J [w_{j,k,u}]_{u=1}^U \cdot z_{j,k} \cdot [\mathbf{x}_n]_j \right) \right) \quad (6)$$

where  $[w_{j,k,u}]_{u=1}^U$  denotes the vector concatenation of the set  $\{w_{j,k,u}\}_{u=1}^U$ , and  $[\xi_n]_k \in \text{one\_hot}(U)$ . On the other

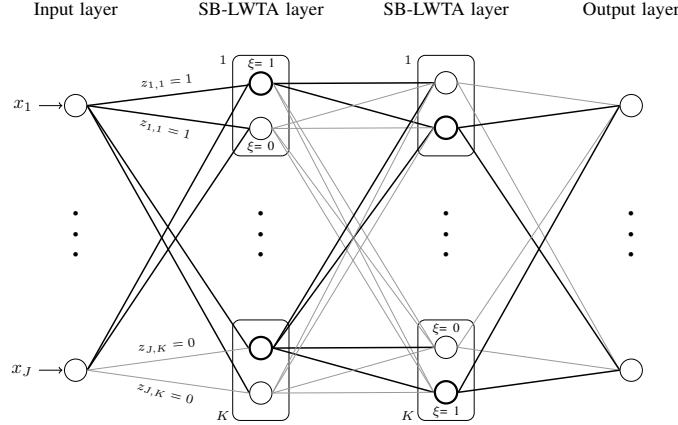


Figure 1. A graphical illustration of the proposed architecture. Bold edges denote active (retained) connections (with  $z = 1$ ); nodes with bold contours denote winner units (with  $\xi = 1$ ); rectangles denote LWTA blocks. We consider  $U = 2$  competitors in each LWTA block,  $k = 1, \dots, K$ .

hand, the utility latent variables,  $\mathbf{Z}$ , are independently drawn from Bernoulli posteriors that read:

$$q(z_{j,k}) = \text{Bernoulli}(z_{j,k} | \tilde{\pi}_{j,k}) \quad (7)$$

where the  $\tilde{\pi}_{j,k}$  are obtained through model training (Section 3.2).

Turning to the prior specification of the model latent variables, we consider a symmetric Discrete prior over the winner unit indicators,  $[\xi_n]_k \sim \text{Discrete}(1/U)$ , and an IBP prior over the utility indicators:

$$u_k \sim \text{Beta}(\alpha, 1) \quad \pi_k = \prod_{i=1}^k u_i \quad z_{j,k} \sim \text{Bernoulli}(\pi_k) \quad \forall j. \quad (8)$$

Finally, we define a distribution over the weight matrices,  $\mathbf{W}$ . To allow for simplicity, we impose a spherical prior  $\mathbf{W} \sim \prod_{j,k} \mathcal{N}(w_{jk} | 0, 1)$ , and seek to infer a posterior distribution  $q(\mathbf{W}) = \prod_{j,k} \mathcal{N}(w_{jk} | \mu_{jk}, \sigma_{jk}^2)$ .

This concludes the formulation of a layer of the proposed SB-LWTA model.

### 3.1. A Convolutional Variant

Further, we consider a variant of SB-LWTA which allows for accommodating convolutional operations. These are of importance when dealing with signals of 2D structure, e.g. images. To perform a convolution operation over an input tensor  $\{\mathbf{X}\}_{n=1}^N \in \mathbb{R}^{H \times L \times C}$  at a network layer, we define a set of kernels, each with weights  $\mathbf{W}_k \in \mathbb{R}^{h \times l \times C \times U}$ , where  $h, l, C, U$  are the kernel height, length, number of channels, and number of competing feature maps, respectively, and  $k \in \{1, \dots, K\}$ . Hence, contrary to the grouping of linear units in LWTA blocks in Fig. 1, the proposed convolutional

variant performs local competition among feature maps. That is, each (convolutional) kernel is treated as an LWTA block. Each layer of our convolutional SB-LWTA networks comprises multiple kernels of competing feature maps.

We provide a graphical illustration of the proposed convolutional variant of SB-LWTA in Fig. 2. Under this model variant, we define the utility latent indicator variables,  $z$ , over whole kernels, that is full LWTA blocks. If the inferred posterior,  $q(z_k = 1)$ , over the  $k$ th block is low, then the block is essentially removed from the network. Our insights motivating this modeling selection concern the resulting computational complexity. Specifically, this formulation allows for completely removing kernels, thus *reducing* the number of executed convolution operations. Hence, this construction facilitates efficiency, since convolution is computationally expensive.

Under this rationale, a layer of the proposed convolutional variant represents an input,  $\mathbf{X}_n$ , with an output tensor  $\mathbf{Y}_n \in \mathbb{R}^{H \times L \times K \times U}$  obtained as the concatenation along the last dimension of the subtensors  $\{[\mathbf{Y}_n]_k\}_{k=1}^K \in \mathbb{R}^{H \times L \times U}$  defined below:

$$[\mathbf{Y}_n]_k = [\xi_n]_k ((\mathbf{W}_k \cdot z_k) \star \mathbf{X}_n) \quad (9)$$

where “ $\star$ ” denotes the convolution operation and  $[\xi_n]_k \in \text{one\_hot}(U)$ . Local competition among *feature maps within an LWTA block (kernel)* is implemented via a sampling procedure which is driven from the feature map output, yielding:

$$q([\xi_n]_k) = \text{Discrete}([\xi_n]_k | \text{softmax}(\sum_{h', l'} [z_k \mathbf{W}_k \star \mathbf{X}_n]_{h', l', u})) \quad (10)$$

We postulate a prior  $[\xi_n]_k \sim \text{Discrete}(1/U)$ . We consider

$$q(z_k) = \text{Bernoulli}(z_k | \tilde{\pi}_k) \quad (11)$$

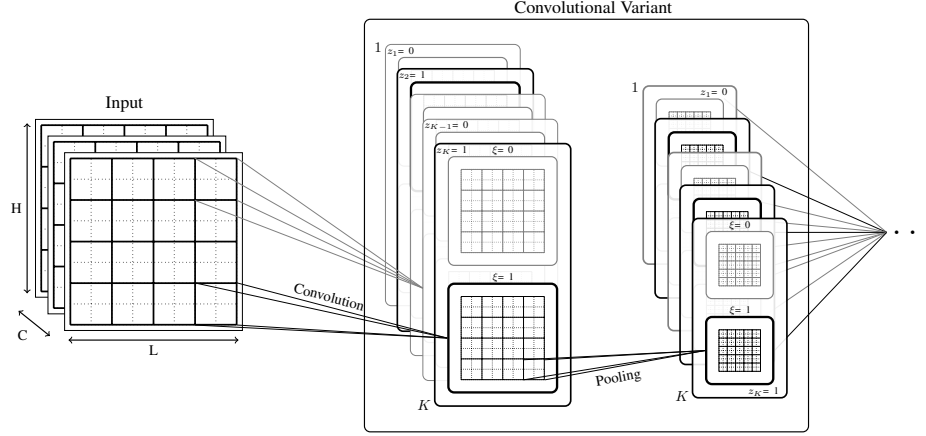


Figure 2. A convolutional variant of our approach. Bold frames denote active (retained) kernels (LWTA blocks of competing feature maps), with  $z = 1$ . Bold rectangles denote winner feature maps (with  $\xi = 1$ ).

with corresponding priors:

$$u_k \sim \text{Beta}(\alpha, 1) \quad \pi_k = \prod_{i=1}^k u_i \quad z_k \sim \text{Bernoulli}(\pi_k) \quad (12)$$

Finally, we again consider network weights imposed a spherical prior  $\mathcal{N}(0, 1)$ , and seek to infer a posterior distribution of the form  $\mathcal{N}(\mu, \sigma^2)$ .

### 3.2. Model Training

To train the proposed model, we resort to maximization of the resulting ELBO expression. Specifically, we adopt SGVB combined with: (i) the standard reparameterization trick for the postulated Gaussian weights,  $\mathbf{W}$ , (ii) the Gumbel-Softmax relaxation trick (Maddison et al., 2017) for the introduced latent indicator variables,  $\xi$  and  $\mathbf{Z}$ ; and (iii) the Kumaraswamy reparameterization trick (Kumaraswamy, 1980) for the stick variables  $v$ . We introduce the mean-field (posterior independence) assumption across layers, as well as among the latent variables  $\xi$  and  $\mathbf{Z}$  pertaining to the same layer. All the posterior expectations in the ELBO<sup>1</sup> are computed by drawing MC samples under the Normal, Gumbel-Softmax and Kumaraswamy repametrization tricks respectively. Then, ELBO maximization is performed using standard off-the-shelf, stochastic gradient techniques; specifically, we adopt ADAM (Kingma & Ba, 2014) with default settings.

### 3.3. Inference Algorithm

Having trained the model posteriors, we can now use them to effect inference for unseen data. In this context, SB-LWTA offers two main advantages over conventional techniques:

<sup>1</sup>The resulting ELBO expressions are provided in the supplementary material.

(i) By exploiting the inferred component utility latent indicator variables, we can naturally devise a method for removing components that are effectively deemed redundant. To this end, one may introduce a *cut-off threshold*,  $\tau$ ; any component with inferred corresponding posterior  $q(z)$  below  $\tau$  is removed from the network. We emphasize that this mechanism is in stark contrast to recent related work in the field of BNNs; in these cases, utility is only implicitly inferred, by thresholding higher-order moments of hierarchical densities over the values of the *network weights themselves*,  $\mathbf{W}$  (see also related discussion in Sec. 1). For instance, (Louizos et al., 2017) recently proposed imposing the following prior over the network weights

$$z \sim p(z) \quad w \sim \mathcal{N}(0, z^2) \quad (13)$$

where  $p(z)$  can be a Horseshoe-type or log-uniform prior. It becomes apparent that the interpretation of connection utility under this prior configuration is open to subjectivity. Besides, its very design, especially when it comes to selection of the prior  $p(z)$ , entails quite an artistry from the side of the practitioners.

(ii) The provision of a full Gaussian posterior distribution over the network weights,  $\mathbf{W}$ , offers a natural way of reducing the floating-point bit precision level of the network implementation. Specifically, the posterior variance of the network weights constitutes a measure of uncertainty in their estimates. Therefore, we can leverage this uncertainty information to assess which bits are significant, and remove the ones which fluctuate too much under approximate posterior sampling. The unit round off necessary to represent the weights is computed by making use of the mean of the weight variances, in a fashion similar to Louizos et al. (2017).

We emphasize that, contrary to Louizos et al. (2017), our



model is endowed with the important benefit that the procedure of bit precision selection for the network weights relies on different posteriors than the component omission process. We posit that by disentangling these two processes, we reduce the tendency of the model to underestimate posterior variance. Thus, we may yield stronger network compression while retaining predictive performance.

Finally, we turn to prediction generation. To be Bayesian, we need to sample several configurations of the weights in order to assess the predictive density, and perform averaging; this is inefficient for real-world testing. Here, we adopt a common approximation as in (Louizos et al., 2017; Neklyudov et al., 2017); that is, we perform traditional forward propagation using the means of the weight posteriors in place of the weight values.

## 4. Experimental Evaluation<sup>2</sup>

In the following, we evaluate the two proposed variants of our SB-LWTA approach on different benchmarks. We assess the predictive performance of the model and its compression<sup>3</sup> and pruning effectiveness. We also compare the effectiveness of local competition among linear units to standard nonlinearities that entail no local competition.

### 4.1. Implementation Details

Throughout our experiments, the stick variables are drawn from a Beta(1, 1) prior. The innovation parameters,  $\alpha$ , of the approximate posterior Kumaraswamy distributions of the sticks are initialized at the number of LWTA blocks of their corresponding layer. All other initializations are random within the corresponding support sets. The employed cut-off threshold,  $\tau$ , is set to  $10^{-2}$ . We emphasize that the evaluated simple SB-LWTA networks remove *connections* on the basis of the corresponding latent indicators  $z$  being below the set threshold  $\tau$ . Analogously, when using the proposed convolutional SB-LWTA architecture, we remove full LWTA *blocks* (convolutional kernels).

### 4.2. Experimental results

We first consider the classical LeNet-300-100 feedforward architecture. We initially explore the potency of LWTA nonlinearities regarding their classification performance and bit precision requirements, compared to using ReLU and Maxout (Goodfellow et al., 2013) activations, when employed in the same setting. To this end, we replace the  $K$  LWTA blocks and the  $U$  units therein (Fig. 1) with (i)  $K$  max-

Table 1. Classification accuracy and bit precision for the LeNet-300-100 architecture. No connection pruning is performed. Bit precision refers to the necessary precision (in bits) required to represent the weights of each of the three layers.

ACTIVATION	ERROR(%)	BIT PRECISION (ERROR %)
RELU	1.60	2/4/10 (1.62)
MAXOUT/2 UNITS	1.38	1/3/12 (1.57)
MAXOUT/4 UNITS	1.67	2/5/12 (1.75)
SB-LWTA/2 UNITS	<b>1.31</b>	1/3/11 (1.47)
SB-LWTA/4 UNITS	1.34	<b>1/2/8</b> (1.5)

out blocks, each comprising  $U$  units, and (ii)  $K \cdot U$  ReLU units (see supplementary material); no other regularization techniques were used, e.g., dropout layers. Training is performed by resorting to Bayes-by-back-prop (Blundell et al., 2015). That is, we impose Gaussian priors over the weights and infer the corresponding posteriors. We utilize SGVB combined with the reparameterization trick, similar to our approach. We then examine the sparsity dynamics induced by the IBP-based mechanism and the competition patterns between the LWTA units. We consider two alternative configurations comprising: 1) 150 and 50 LWTA blocks on the first and second layer, respectively, of two competing units each, and 2) 75 and 25 LWTA blocks of four competing units. This allows for us to examine the effect of the number of competing LWTA units on model performance, *with all competitors initialized at the same number of weights*. We use the MNIST dataset in all these experiments.

Further, we consider the LeNet-5-Caffe<sup>4</sup> convolutional net, which we also evaluate on MNIST. The original LeNet-5-Caffe comprises a 5x5 kernel with 20 feature maps on the first layer, a 5x5 kernel with 50 feature maps on the second layer and a dense layer with 500 units on the third. In our (convolutional) SB-LWTA implementation, we consider 10 5x5 kernels (LWTA blocks) on the first layer, and 25 5x5 kernels on the second layer, with 2 competing feature maps each. We additionally consider an implementation comprising 4 competing feature maps with 5 5x5 kernels on the first layer, and 12 5x5 kernels on the second layer, reducing the total feature maps of the second layer to 48; this allows us to split to even LWTA blocks comprising 4 competing feature maps each.

Finally, we perform experimental evaluations on a more challenging benchmark dataset, namely CIFAR-10 (Krizhevsky & Hinton, 2009). In this context, and due to hardware limitations, we employ a simple convolutional architecture, dubbed ConvNet, following the one proposed by Alex Krizhevsky<sup>5</sup> instead of the usual VGG-like architecture provided in (Louizos et al., 2017). The architecture comprises two 5x5 kernel with 64 feature maps convolutional layers, followed by two dense layers with 384 and 192

<sup>2</sup>We have developed our source codes in Python, using TensorFlow (Abadi et al., 2015)

<sup>3</sup>For calculating the needed bit precision, we exploit the script provided in: [https://github.com/KarenUllrich/Tutorial\\_BayesianCompressionForDL](https://github.com/KarenUllrich/Tutorial_BayesianCompressionForDL)

<sup>4</sup><https://github.com/BVLC/caffe/tree/master/examples/mnist>

<sup>5</sup><https://code.google.com/archive/p/cuda-convnet/>

Table 2. Pruned LeNet 300-100 Architectures. In this table, SB-ReLU denotes a variant of our proposed approach where we replace LWTA blocks with ReLU units.

Architecture	Method	Error (%)	# Weights	Bit precision
LeNet 300-100	Original	1.6	235K/30K/1K	23/23/23
	StructuredBP (Neklyudov et al., 2017)	1.7	23,664/6,120/450	23/23/23
	Sparse-VD (Molchanov et al., 2017)	1.92	58,368/8,208/720	8/11/14
	BC-GHS (Louizos et al., 2017)	1.8	26,746/1,204/140	13/11/10
	SB-ReLU	1.75	13,698/6,510/730	3/4/11
	SB-LWTA (2 units)	1.7	12,522/6,114/534	2/3/11
	SB-LWTA (4 units)	1.75	23,328/9,348/618	2/3/12

units respectively. Similar to LeNet-5-Caffe, our SB-LWTA implementation consists in splitting the original architecture into pairs of competing feature maps on each layer.

**LeNet-300-100.** We train the network from scratch on the MNIST dataset, without using any data augmentation procedure. In Table 1, we compare the classification performance of our approach, employing 2 or 4 competing LWTA units, to LeNet-300-100 configurations employing commonly used nonlinearities. The results reported in this Table pertaining to our approach, are obtained without removing connections the utility posteriors,  $q(z)$ , of which fall below the cut-off threshold,  $\tau$ . In the second column of this Table, we observe that our SB-LWTA model offers competitive accuracy and improves over the considered alternatives when operating at full bit precision (float32). The third column of this Table shows how network performance changes when we attempt to reduce bit precision for both our model and the considered competitors<sup>6</sup>. Bit precision reduction is based on the inferred weight posterior variance, as explained in the supplementary material. As we observe, not only does our approach yield a clearly improved accuracy in this case, but it also imposes the lowest memory footprint.

The corresponding comparative results obtained when we employ the considered threshold to remove connections and induce sparsity in our model are depicted in Table 2. As we observe, our approach continues to yield competitive accuracy; this is on par with the best performing alternative, which requires, though, a significantly higher number of weights combined with up to an order of magnitude higher bit precision. Thus, our approach yields the same accuracy for a lighter memory footprint. Indeed, it is important to note that our approach remains at the top of the list in terms of the obtained accuracy while retaining the *least number of weights*, despite the fact that it was initial-

<sup>6</sup>Following the IEEE 754-2008 convention, the representation of floating-point data in the binary interchange formats, considers 3 different quantities: a) 1-bit sign, b)  $w$  exponent bits and c)  $t = p - 1$  precision in bits (Zuras et al., 2008). For the 32-bit format,  $p = 24$ , and thus we report the value  $t = 23$  as the original bit precision.

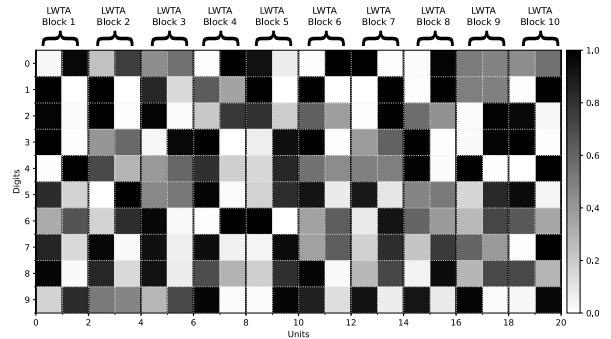


Figure 3. Probabilities of unit activations for each digit in the test set for the first 10 blocks of the second layer of the LeNet-300-100 network. LWTA blocks comprise two competing units; Black denotes very high activation probability, while white denotes that the probability of activation is very low.

ized in the same dense fashion as the alternatives. Even more importantly, our method *completely outperforms all the alternatives* when it comes to its final bit precision requirements.

Finally, it is significant to note that by replacing in our model the LWTA blocks with ReLU units, a variant we dub SB-ReLU in Table 2, we yield clearly inferior performance when it comes to network pruning and weight compression, combined with a slightly inferior accuracy. This offers strong evidence that LWTA mechanisms, at least the way implemented in our work, offer benefits over conventional nonlinearities.

**LeNet-5-Caffe and ConvNet convolutional architectures.** For the LeNet-5-Caffe architecture, we train the network from scratch. In Table 3, the obtained comparative effectiveness of our approach, employing 2 or 4 competing LWTA feature maps; both the classification performance and network pruning and compression are depicted. Our approach requires the *least number of feature maps* while at the same time offering significantly *higher compression rates* in terms of bit precision, as well as better classification accuracy than the best considered alternative. By using the SB-ReLU variant of our approach, we once again yield inferior performance compared to SB-LWTA, both in

Table 3. Learned (Pruned) Convolutional Architectures.

Architecture	Method	Error (%)	# Feature Maps (Conv. Layers)	Bit precision (All Layers)
LeNet-5-Caffe	Original	0.9	25/50	23/23/23/23
	StructuredBP (Neklyudov et al., 2017)	0.86	3/18	23/23/23/23
	Sparse-VD (Molchanov et al., 2017)	1.0	14/19	13/10/8/12
	BC-GHS (Louizos et al., 2017)	1.0	5/10	10/10/14/13
	SB-ReLU	0.9	10/16	8/3/3/11
	SB-LWTA-2	0.9	6/6	6/3/3/13
	SB-LWTA-4	0.8	8/12	11/4/1/11
ConvNet	Original	17.0	64/64	23 in all layers
	BC-GNJ(Louizos et al., 2017)	18.6	54/49	13/8/4/5/12
	BC-GHS(Louizos et al., 2017)	17.9	42/52	12/8/5/6/10
	SB-LWTA-2	17.5	40/42	11/7/5/4/10

terms of network pruning and compression, reaffirming the benefits of LWTA mechanisms compared to conventional nonlinearities.

For the considered ConvNet architecture, we initially train the model with LWTA activations without incorporating the sparsity inducing mechanism. The model is trained for 200 epochs and we use the pretrained weights to fine-tune the full model by activating inference of component utility and network pruning. This approach is common in the related literature; for instance, (Louizos et al., 2017), consistently observed a performance improvement of 1%-2% in terms of predictive accuracy. We additionally implement the BC-GNJ and BC-GHS models with the default parameters as described in (Louizos et al., 2017) in order to compare the predictive, pruning and compression performance of our approach. The learned architectures along with their classification accuracy and bit precision requirements are illustrated in Table 3. Similarly to the LeNet-5-Caffe convolutional architecture, our method retains the *least number of feature maps*, while at the same time provides the *most competitive bit precision requirements* accompanied by *higher predictive accuracy* compared to the competition.

**Further Insights.** Finally, we examine the activation patterns of the competing units in the LWTA blocks of an SB-LWTA network. To this end, we focus on the second layer of the LeNet-300-100 network with LWTA blocks comprising two competing units. Initially, we examine the distribution of the unit activation probabilities of the network’s LWTA blocks, and how they vary over the ten MNIST classes. In Figure 3, we depict the probabilities of unit activation for all the digits in MNIST for the first 10 LWTA blocks, averaged over all data points in the test set. As we observe, the distribution of unit activation probabilities is essentially different between any pair of digits. This provides strong evidence that the LWTA activation mechanism succeeds in learning to encode distinct fundamental patterns in the observed data. Further, in Figure 4, we examine what the overlap of unit activation is among the MNIST digits. Specifically, for

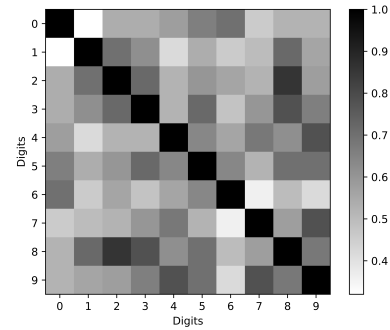


Figure 4. Fractions of overlapping activated units for each pair of digits. Black denotes that all activated units are the same; moving towards the white spectrum, unit activation overlap drops.

each digit, we compute the most often activated unit in each LWTA block and derive the fraction of overlapping activated units over all blocks, for each pair of digits. It is apparent that, the unit activation overlap is quite low, typically below 50%. Therefore, upon switching between digits, at least 50% of the network changes its LWTA unit activation.

## 5. Conclusions

In this paper, we introduced a new deep network design principle that allows for obtaining less parameterized networks with reduced memory footprint without compromising the obtainable accuracy. To this end, we utilized LWTA nonlinearities, and sparsity inducing priors based on the IBP. Our experiments have provided strong evidence that our approach offers significantly *more vigorous pruning* of the considered networks combined with state-of-the-art accuracy and compression. Note also that the postulated local competition mechanisms yielded significantly different unit activation patterns among observations belonging to distinct classes. In our future work, we intend to examine how our networks can be helpful in transfer learning problems, especially when dealing with online learning problems.



## References

- Abadi, M. et al. TensorFlow: Large-scale machine learning on heterogeneous systems, 2015. Software available from tensorflow.org.
- Andersen, P., Gross, G. N., Lomo, T., and Sveen, O. Participation of inhibitory and excitatory interneurons in the control of hippocampal cortical output. *UCLA Forum Med Sci*, 11:415–465, 1969.
- Ba, J. and Caruana, R. Do deep nets really need to be deep? In *Proc. NIPS 27*, pp. 2654–2662, 2014.
- Blundell, C., Cornebise, J., Kavukcuoglu, K., and Wierstra, D. Weight uncertainty in neural networks. *arXiv preprint arXiv:1505.05424*, 2015.
- Chatzis, S. Indian buffet process deep generative models for semi-supervised classification. In *IEEE ICASSP*, 2018.
- Douglas, R. J. and Martin, K. A. Neuronal circuits of the neocortex. *Annu. Rev. Neurosci.*, 27:419–451, 2004.
- Eccles, J. C., Szentagothai, J., and Ito, M. *The cerebellum as a neuronal machine*. Springer-Verlag, 1967.
- Gal, Y. and Ghahramani, Z. Dropout as a Bayesian approximation: Representing model uncertainty in deep learning. *arXiv:1506.02142*, 2015.
- Goodfellow, I. J., Warde-Farley, D., Mirza, M., Courville, A., and Bengio, Y. Maxout networks. In *Proc. ICML-Volume 28, ICML 13*, pp. III–1319–III–1327, 2013.
- Graves, A. Practical variational inference for neural networks. In *Proc. NIPS*, pp. 2348–2356, 2011.
- Griffiths, T. L. and Ghahramani, Z. Infinite latent feature models and the indian buffet process. In *Proc. NIPS*, pp. 475–482. MIT Press, 2005.
- Grossberg, S. The art of adaptive pattern recognition by a self-organizing neural network. *Computer*, pp. 77–88, 1988.
- Hinton, G., Vinyals, O., and Dean, J. Distilling the knowledge in a neural network. In *NIPS Deep Learning and Representation Learning Workshop*, 2015.
- Ishwaran, H. and James, L. F. Gibbs sampling methods for stick-breaking priors. *Journal of the American Statistical Association*, 96(453):161–173, 2001. ISSN 01621459.
- Jang, E., Gu, S., and Poole, B. Categorical reparameterization using gumbel-softmax. In *Proc. ICLR*, 2017.
- Kandel, E. R., Schwartz, J. H., and Jessell, T. M. (eds.). *Principles of Neural Science*. Elsevier, New York, third edition, 1991.
- Kingma, D. P. and Ba, J. Adam: A method for stochastic optimization. *arXiv preprint arXiv:1412.6980*, 2014.
- Kingma, D. P. and Welling, M. Auto-encoding variational Bayes. In *Proc. ICLR*, 2014.
- Krizhevsky, A. and Hinton, G. Learning multiple layers of features from tiny images. Technical report, 2009.
- Kumaraswamy, P. A generalized probability density function for double-bounded random processes. *Journal of Hydrology*, 46(1):79 – 88, 1980. ISSN 0022-1694. doi: [https://doi.org/10.1016/0022-1694\(80\)90036-0](https://doi.org/10.1016/0022-1694(80)90036-0).
- Lansner, A. Associative memory models: from the cell-assembly theory to biophysically detailed cortex simulations. *Trends in Neurosciences*, 32(3):178 – 186, 2009. ISSN 0166-2236. doi: <https://doi.org/10.1016/j.tins.2008.12.002>.
- LeCun, Y., Bengio, Y., and Hinton, G. Deep learning. *Nature*, 521(7553):436, 2015.
- Lee, D. D. and Seung, H. S. Learning the parts of objects by nonnegative matrix factorization. *Nature*, 401:788–791, 1999.
- Louizos, C., Ullrich, K., and Welling, M. Bayesian compression for deep learning. In *Proc. NIPS*, pp. 3290–3300, 2017.
- Maass, W. Neural computation with winner-take-all as the only nonlinear operation. In *Proc. NIPS 12*, pp. 293–299, Cambridge, MA, USA, 1999. MIT Press.
- Maass, W. On the computational power of winner-take-all. *Neural Comput*, 12(11):2519–2535, Nov 2000.
- Maddison, C. J., Mnih, A., and Teh, Y. W. The concrete distribution: A continuous relaxation of discrete random variables. In *Proc. ICLR*, 2017.
- McCloskey, M. and Cohen, N. J. Catastrophic interference in connectionist networks: The sequential learning problem. volume 24 of *Psychology of Learning and Motivation*, pp. 109 – 165. Academic Press, 1989. doi: [https://doi.org/10.1016/S0079-7421\(08\)60536-8](https://doi.org/10.1016/S0079-7421(08)60536-8).
- Molchanov, D., Ashukha, A., and Vetrov, D. Variational dropout sparsifies deep neural networks. In *Proc. ICML 34*, volume 70 of *Proc. MLR*, pp. 2498–2507, International Convention Centre, Sydney, Australia, 06–11 Aug 2017. PMLR.
- Nalisnick, E. and Smyth, P. Stick-breaking variational autoencoders. In *Proc. ICLR*, 2016.
- Neklyudov, K., Molchanov, D., Ashukha, A., and Vetrov, D. P. Structured bayesian pruning via log-normal multiplicative noise. In *Proc. NIPS 31*, pp. 6775–6784, 2017.

- Olshausen, B. A. and Field, D. J. Emergence of simple-cell receptive field properties by learning a sparse code for natural images. *Nature*, 381(6583):607–609, Jun 1996.
- Srivastava, R. K., Masci, J., Kazerounian, S., Gomez, F., and Schmidhuber, J. Compete to compute. In *Proc. NIPS 26*, pp. 2310–2318. Curran Associates, Inc., 2013.
- Stefanis, C. Interneuronal mechanisms in the cortex. *UCLA Forum Med Sci*, 11:497–526, 1969.
- Teh, Y. W., Görür, D., and Ghahramani, Z. Stick-breaking construction for the Indian buffet process. In *Proc. AIS-TATS*, volume 11, 2007.
- Zuras, D., Cowlshaw, M., Aiken, A., Applegate, M., Bailey, D., Bass, S., Bhandarkar, D., Bhat, M., Bindel, D., Boldo, S., Canon, S., Carlough, S. R., Cornea, M., Cowlshaw, M., Crawford, J. H., Darcy, J. D., Das Sarma, D., Dumas, M., Davis, B., Davis, M., Delp, D., Demmel, J., Erle, M. A., Fahmy, H. A. H., Fasano, J. P., Fateman, R., Feng, E., Ferguson, W. E., Fit-Florea, A., Fournier, L., Freitag, C., Godard, I., Golliver, R. A., Gustafson, D., Hack, M., Harrison, J. R., Hauser, J., Hida, Y., Hinds, C. N., Hoare, G., Hough, D. G., Huck, J., Hull, J., Ingrassia, M., James, D. V., James, R., Kahan, W., Kapernick, J., Karpinski, R., Kidder, J., Koev, P., Li, R.-C., Liu, Z. A., Mak, R., Markstein, P., Matula, D., Melquiond, G., Mori, N., Morin, R., Nedialkov, N., Nelson, C., Oberman, S., Okada, J., Ollmann, I., Parks, M., Pittman, T., Postpischil, E., Riedy, J., Schwarz, E. M., Scott, D., Senzig, D., Sharapov, I., Shearer, J., Siu, M., Smith, R., Stevens, C., Tang, P., Taylor, P. J., Thomas, J. W., Thompson, B., Thrash, W., Toda, N., Trong, S. D., Tsai, L., Tsen, C., Tydeman, F., Wang, L. K., Westbrook, S., Winkler, S., Wood, A., Yalcinalp, U., Zemke, F., and Zimmermann, P. IEEE Standard for Floating-Point Arithmetic. Technical report, IEEE, August 2008.